Optical spectra and thermal Schottky levels in dysprosium sesquisulfide

John B. Gruber[a)]
Department of Physics, San Jose State University, San Jose, California 95192-0106

Bahram Zandi
Army Research Laboratory/Sensors and Electron Devices Directorate, 2800 Powder Mill Road, Adelphi, Maryland 20783-1197

Bruce Justice and Edgar F. Westrum, Jr.
Department of Chemistry, University of Michigan, Ann Arbor, Michigan 48109-1055

(Received 11 January 1999; accepted 26 March 1999)

We report a detailed crystal-field splitting analysis of the energy levels of $Dy^{3+}(4f^9)$ in single crystals of Dy_2S_3 that have the Th_3P_4 cubic defect structure. From an analysis of the temperature-dependent absorption spectra, we have identified seven of the eight crystal-field split energy (Stark) levels of the ground-state multiplet manifold, $^6H_{15/2}$. Sixty-two experimental Stark levels from various multiplet manifolds of Dy^{3+} are compared with a calculated crystal-field splitting, whose initial crystal-field parameters, B_{nm}, were determined from lattice-sum calculations. The rms deviation between experimental and calculated levels is 7 cm^{-1}. Both the experimental and calculated crystal-field splitting of the $^6H_{15/2}$ manifold are compared with an assignment of Schottky levels obtained from a reassessment of heat capacity data reported earlier. Based on entropy considerations and verification of the Schottky level assignments by analyses of the optical and magnetic susceptibility data, we conclude that the anomaly observed in the heat capacity data near 3.4 K is due to antiferromagnetic ordering. © *1999 American Institute of Physics.* [S0021-9606(99)70424-1]

I. INTRODUCTION

The optical, magnetic, and thermophysical properties of the lanthanide sesquisulfides (Ln_2S_3) are important since these materials have been used successfully as components in advanced thermoelectrical, solar photovoltaic, and infrared sensor/detector devices.[1–3] Although Ln_2S_3 exists in several phases, it is the Th_3P_4 defect structure (commonly called the γ-phase) that manifests the most interesting physical properties due to the considerable variation in composition that can be obtained during its chemical preparation.[4–7] Since one-ninth of the cation positions in the γ-phase structure are randomly unoccupied, these positions can be filled with excess Ln cations forming a solid solution without a change in the crystal structure.[8–10] Superconducting, semiconducting, and insulator behavior have been reported over a cation composition range Ln_3S_4–Ln_2S_3, which provides for a remarkable study on the role that the $4f$ electrons play in these materials.[11–14]

Over the years, several groups have reported some of the thermophysical properties of the lanthanide sesquisulfides.[15–17] One of the most complete studies was carried out by Westrum and his co-workers.[18–20] Their interpretations were strengthened when analyses of optical and magnetic data were also available to support the Schottky level assignments deduced from analyses of the heat capacity data.[21–23] The success of these comparative studies depended on making measurements on samples of similar composition. Such an integrated view of the optical, magnetic, and thermophysical properties was obtained for γ-phase Ce_2S_3 and Nd_2S_3.[18] The purpose of this study is to provide a similar perspective for γ-phase Dy_2S_3.

Low temperature (2 to 20 K) calorimetric measurements on γ-phase Dy_2S_3 reported by Taher *et al.*[17] show a ''bump'' on the heat capacity curve near 3.4 K. The authors attributed this bump to Schottky levels rather than to cooperative phenomena. Calorimetric measurements made by Westrum and his group between 5 and 350 K on samples of similar composition could not be reconciled to this explanation.[19] Based on entropy considerations, they proposed that the anomaly was likely due to magnetic ordering. Paramagnetic susceptibility data obtained from the Westrum samples between 2 and 350 K indicated that antiferromagnetic ordering takes place around 3.4 K.[24] However, establishing the low-energy Schottky levels is complicated by the residue of magnetic ordering that contributes to the overall heat capacity observed above 5 K in the Dy_2S_3 samples. Moreover, the optical spectra reported by Taher *et al.*[17] was obtained at temperatures too low to verify the Schottky-level assignments reported by the Westrum group.[19]

To resolve these differences, and to establish an independent experimental basis for establishing the Schottky levels, we report a detailed crystal-field splitting analysis of the Dy^{3+} ion-energy levels in γ-phase Dy_2S_3, having the same composition as the samples used in measuring the heat capacity data. Sixty-two experimental energy (Stark) levels identified from the optical spectra of various multiplet manifolds, $^{2S+1}L_J$, of $Dy^{3+}(4f^9)$ are compared with a calculated crystal-field splitting, whose initial crystal-field parameters,

a)Electronic mail: jbgruber@email.sjsu.edu

B_{nm}, were determined from lattice-sum calculations. The rms deviation between the experimental and calculated splitting is 7 cm^{-1}.

Both the experimental and calculated crystal-field splitting of the ground-state multiplet manifold of $Dy^{3+}(^6H_{15/2})$ are compared with Schottky levels obtained from a recent reassessment of the heat capacity data of γ-phase Dy_2S_3 measured by both the Taher and Westrum groups.[17,19] Our analysis of the temperature-dependent (hot-band) absorption spectra, confirmed by the crystal-field splitting calculations, is able to verify seven of the eight expected twofold degenerate Schottky levels. The eighth level likely corresponds to the highest-energy Stark level in the $^6H_{15/2}$ manifold that cannot be identified with any certainty from the optical data.

II. SPECTROSCOPIC MEASUREMENTS

The samples investigated in the present study were grown by Henderson and Johnson in the late sixties.[25] Optically transparent crystals, retaining a yellow-green color, were produced by diffusing sulfur into the crystals at 1200 °C. X-ray crystallography carried out on the samples indicated that the structure was the high-temperature (γ-phase) Th_3P_4, and sample compositions were determined to be $DyS_{1.500\pm0.001}$ from chemical analyses.[25] The samples used in the present optical studies have the same composition as the samples used by Taher *et al.*[17] and Westrum *et al.*[18,19,24]

The absorption spectrum reported in Table I was taken by J. B. Gruber at Portland State University[26] with a Cary model 14 spectrophotometer that covered the wavelength range between 2500 and 400 nm. A conduction dewar filled with liquid nitrogen provided sample temperatures between 85 K and room temperature. Paramagnetic susceptibility data[24] on samples of similar composition indicate that $\gamma-Dy_2S_3$ is paramagnetic over the temperature range investigated spectroscopically, so that the temperature-dependent transitions (hot-band absorption spectra) establish levels that can be compared directly to the Schottky levels reported earlier.[18–20]

Table I reports the absorption spectrum and the energy levels of $Dy^{3+}(4f^9)$ in γ-phase Dy_2S_3 obtained at approximately 85 K. The hot-band spectra observed at this temperature from the first excited Stark level at 52 cm^{-1} have been excluded from the table in order to simplify the presentation of the transitions to various individual multiplet manifolds. Although somewhat broader and shifted to lower energies, the spectrum in Table I is similar to the absorption spectrum reported at 10 K by Taher *et al.*[17] for multiplet manifolds $^4I_{15/2}$, $^4F_{9/2}$, $^6F_{3/2}$, and $^6F_{7/2}$. In fact, the close agreement provides support in identifying the hot bands observed between 85 K and room temperature, which is an important part of the present study.

From the hot-band data we have identified temperature-dependent transitions from the Stark levels of the ground-state multiplet manifold, $^6H_{15/2}$ to excited mulitplet manifolds. Hot-band spectra associated with quartet states $^4F_{9/2}$, $^4I_{15/2}$, and $^4G_{11/2}$ provide the most complete pattern of data. For example, the lowest-energy Stark level of the $^4G_{11/2}$ observed at 430.5 nm (23 224 cm^{-1}) in Table I has a pattern of hot bands identified at room temperature as 431.4 nm (23 172 cm^{-1}), 433.1 nm (23 084 cm^{-1}), 434.0 nm (23 034 cm^{-1}), 434.9 nm (22 984 cm^{-1}), 435.5 nm (22 967 cm^{-1}), and 436.3 nm (22 914 cm^{-1}). From this pattern, seven of eight expected doubly degenerate Stark levels are identified at 0, 52, 140, 190, 240, 257, and 310, all in energy units of cm^{-1}. These levels are listed in Table II. Additional hot-band data involving other excited multiplets establish a similar pattern of splitting and are available as supplemental material from the authors. The temperature-dependent data are too broad to confirm any Stark levels between 4 and 6 cm^{-1} above the ground-state Stark level, and the 44 cm^{-1} level reported by Taher *et al.*[17] appears to be shifted in the present study to a somewhat higher energy. Polarized absorption spectra are not observed. In the defect cubic structure, the cation symmetry axes can point along either the $\hat{x}$, $\hat{y}$, or $\hat{z}$ directions. No fluorescence was observed. Very likely, quenching of the fluorescence takes place in the undiluted single crystals of γ-phase Dy_2S_3.

III. CRYSTAL-FIELD SPLITTING CALCULATIONS

The crystal-field splitting of the multiplet manifolds reported in Tables I and II was calculated using the crystal-field Hamiltonian

$$H_{\mathrm{cf}}=\sum_{nm} B_{nm}\sum_{i} C_{nm}(\hat{r}_i),$$

where the B_{nm} terms represent the crystal-field parameters with $B_{nm}=(-1)^m B_{n,-m}$, and the $C_{nm}(\hat{r}_i)$ operators are related to the spherical harmonics.[27] The sums over n and m are established by the Dy^{3+} ion symmetry in the lattice, and the sum over i includes the nine $4f$ electrons associated with the ground-state electronic configuration, $Dy^{3+}(4f^9)$. The B_{nm} parameters are considered phenomenological in that they are established by a systematic fitting of a set of calculated Stark (energy) levels to the observed splitting of the multiplet manifolds. We have found, from previous analyses of the spectra of other rare earth ions, that lattice-sum calculations based on the structure and symmetry of ions in the crystal provide an initial set of B_{nm} parameters sufficiently close to the final set of B_{nm} so as to reduce chances for a false minima in the analysis.[28,29]

Kaminskii[30] has formulated arguments and conclusions concerning the symmetry of the lanthanide ions in systems where there is random occupation of the lanthanide ion in defect or charge compensated sites. Structural dynamic disorder in γ-phase Dy_2S_3 leads to the formation of $Dy^{3+}-S^{2-}$ polyhedra having a slightly higher symmetry of D_{2d} as the local symmetry of Dy^{3+} than the S_4 symmetry that is established for the cation sites (vacant and occupied) from x-ray crystallography analyses of single crystals.[31] To test the Kaminskii conclusions for γ-phase Dy_2S_3, we have used the polyhedral symmetry of D_{2d} for our analysis. This choice reduces the number of B_{nm} parameters from six in S_4 symmetry to five in D_{2d} symmetry; yet, with the rotation of coordinate axes, B_{20}, B_{40}, B_{44}, B_{60}, and B_{64}, can be compared directly with corresponding parameters in S_4 symmetry.[27,32,33]

TABLE I. Absorption spectrum and energy levels of Dy^{3+} in Dy_2S_3.[a]

$^{2S+1}L_J$[b]	λ(nm)[c]	I[d]	$E(cm^{-1})_{obs}$[e]	$E(cm^{-1})_{calc}$[f]	Percent mixture of states[g]
$^6H_{11/2}$	1731.5	0.27	5774[h]	5770	$99.5\,^6H_{11/2}+0.36\,^6F_{11/2}+0.06\,^6H_{13/2}$
5918	1709.5	0.18	5848[h]	5851	$99.4\,^6H_{11/2}+0.20\,^6F_{11/2}+0.15\,^6H_{9/2}$
	1689.0	0.10	5918[h]	5911	$99.5\,^6H_{11/2}+0.21\,^6H_{9/2}+0.11\,^6H_{13/2}$
	1683.0	0.05	5940[h]	5942	$99.4\,^6H_{11/2}+0.21\,^6F_{11/2}+0.11\,^6H_{13/2}$
	1671(b)	0.02	5983[h]	5985	$99.3\,^6H_{11/2}+0.48\,^6F_{11/2}+0.12\,^6H_{9/2}$
	1668(sh)	0.01	5992	5996	$99.6\,^6H_{11/2}+0.24\,^6F_{11/2}+0.07\,^6F_{7/2}$
$^6F_{11/2}$	1329.5	0.15	7520[h]	7533	$92.3\,^6F_{11/2}+7.21\,^6H_{9/2}+0.27\,^6H_{11/2}$
7604	1323(b)	0.05	7555[h]	7565	$99.1\,^6F_{11/2}+0.43\,^6H_{11/2}+0.30\,^6H_{9/2}$
	1319(sh)	0.06	7581	7581	$97.9\,^6F_{11/2}+1.81\,^6H_{9/2}+0.15\,^6H_{11/2}$
	1316.3	0.10	7595[h]	7595	$98.3\,^6F_{11/2}+1.50\,^6H_{9/2}+0.05\,^6H_{13/2}$
	1307(b)	0.07	7650[h]	7645	$98.6\,^6F_{11/2}+1.00\,^6H_{9/2}+0.23\,^6H_{11/2}$
	1301(b)	0.03	7684	7676	$93.6\,^6F_{11/2}+5.85\,^6H_{9/2}+0.40\,^6H_{11/2}$
$^6H_{9/2}$	1271.0	0.10	7866[h]	7866	$94.8\,^6H_{9/2}+4.43\,^6F_{11/2}+0.47\,^6F_{9/2}$
7988	1255.5	0.05	7963[h]	7963	$94.9\,^6H_{9/2}+4.27\,^6F_{11/2}+0.31\,^6H_{7/2}$
	1253(sh)	0.03	7975	7974	$96.5\,^6H_{9/2}+2.56\,^6F_{11/2}+0.36\,^6H_{7/2}$
	1237.6	0.05	8078[h]	8081	$97.8\,^6H_{9/2}+1.16\,^6F_{11/2}+0.77\,^6F_{9/2}$
	1236(sh)	0.03	8088	8086	$93.9\,^6H_{9/2}+5.27\,^6F_{11/2}+0.43\,^6H_{7/2}$
$^6F_{9/2}$	1127.3	0.03	8870[h]	8871	$94.3\,^6F_{9/2}+5.02\,^6H_{7/2}+0.50\,^6H_{9/2}$
8918	1124.5	0.06	8890[h]	8878	$98.1\,^6F_{9/2}+1.06\,^6H_{7/2}+0.55\,^6H_{5/2}$
	1120(sh)	0.06	8920	8926	$98.6\,^6F_{9/2}+0.91\,^6H_{7/2}+0.23\,^6H_{5/2}$
	1119.5	0.10	8930[h]	8932	$98.8\,^6F_{9/2}+0.58\,^6H_{7/2}+0.31\,^6H_{5/2}$
	1117(sh)	0.05	8950	8952	$95.9\,^6F_{9/2}+3.04\,^6H_{7/2}+0.73\,^6H_{9/2}$
$^6H_{7/2}$	1078(b)	0.12	9273[h]	9284	$94.3\,^6H_{7/2}+5.14\,^6F_{9/2}+0.27\,^6H_{9/2}$
9388	1068.5	0.06	9356[h]	9343	$96.5\,^6H_{7/2}+1.40\,^6H_{5/2}+1.27\,^6F_{9/2}$
	1056.5	0.10	9462[h]	9450	$96.7\,^6H_{7/2}+1.87\,^6H_{5/2}+0.88\,^6F_{9/2}$
	1053(sh)	0.03	9492	9506	$95.8\,^6H_{7/2}+3.47\,^6F_{9/2}+0.23\,^6H_{5/2}$
$^6H_{5/2}$	9957(b)	0.03	10 040[h]	10 043	$96.7\,^6H_{5/2}+1.45\,^6H_{7/2}+0.90\,^6F_{7/2}$
10 154	983(b)	0.06	10 170[h]	10 172	$96.3\,^6H_{5/2}+1.90\,^6H_{7/2}+1.60\,^6F_{7/2}$
	974(b)	0.02	10 265	10 261	$97.8\,^6H_{5/2}+1.11\,^6F_{7/2}+0.53\,^6F_{9/2}$
$^6F_{7/2}$	915.7	0.22	10 917[h]	10 926	$99.5\,^6F_{7/2}+0.23\,^6H_{5/2}+0.07\,^6H_{9/2}$
10 945	912.6	0.31	10 955[h]	10 953	$98.6\,^6F_{7/2}+1.05\,^6H_{5/2}+0.11\,^6H_{9/2}$
	910.9	0.43	10 975[h]	10 972	$98.3\,^6F_{7/2}+1.45\,^6H_{5/2}+0.11\,^6F_{5/2}$
	909.7	0.10	10 990[h]	10 986	$98.7\,^6F_{7/2}+0.84\,^6H_{5/2}+0.17\,^6H_{9/2}$
$^6F_{5/2}$	812.9	0.03	12 298[h]	12 309	$99.7\,^6F_{5/2}+0.14\,^6H_{7/2}+0.10\,^6F_{7/2}$
12 308	811.4	0.06	12 321[h]	12 316	$99.7\,^6F_{5/2}+0.09\,^6F_{1/2}+0.08\,^6H_{9/2}$
	810.7(sh)	0.03	12 331	12 325	$99.4\,^6F_{5/2}+0.25\,^6H_{7/2}+0.21\,^6F_{3/2}$
$^6F_{3/2}$	760.8	0.04	13 140[h]	13 137	$99.6\,^6F_{3/2}+0.20\,^6F_{5/2}+0.12\,^6H_{5/2}$
13 132	759.4(sh)	0.02	13 165[h]	13 173	$61.7\,^6F_{3/2}+38.0\,^6F_{1/2}+0.14\,^6F_{5/2}$
$^4F_{9/2}$	475.7	0.06	21 015[h]	21 016	$99.9\,^4F_{9/2}+0.12\,^4G_{11/2}+0.4\,^4I_{15/2}$
21 101	475.1	0.10	21 047[h]	21 040	$99.8\,^4F_{9/2}+0.15\,^4G_{11/2}+0.01\,^4I_{15/2}$
	473.9	0.18	21 094[h]	21 098	$99.4\,^4F_{9/2}+0.31\,^4G_{11/2}+0.25\,^4I_{15/2}$
	473.6	0.05	21 109[h]	21 122	$99.8\,^4F_{9/2}+0.12\,^4I_{15/2}+0.09\,^4G_{11/2}$
	471.2	0.06	21 216[h]	21 205	$99.8\,^4F_{9/2}+0.19\,^4G_{11/2}+0.02\,^4I_{15/2}$
$^4I_{15/2}$	456.7	0.10	21 890[h]	21 897	$99.4\,^4I_{15/2}+0.33\,^4G_{11/2}+0.30\,^4F_{9/2}$
22 037	455.8	0.10	21 930[h]	21 928	$99.9\,^4I_{15/2}+0.07\,^4F_{9/2}+0.01\,^4G_{11/2}$
	455.2	0.17	21 962[h]	21 970	$99.7\,^4I_{15/2}+0.31\,^4G_{11/2}+0.01\,^4F_{9/2}$
	454.2	0.05	22 010[h]	22 018	$99.5\,^4I_{15/2}+0.48\,^4G_{11/2}+0.02\,^4F_{9/2}$
	453.0	0.10	22 070[h]	22 069	$99.2\,^4I_{15/2}+0.80\,^4G_{11/2}+0.02\,^4F_{9/2}$
	452.3	0.36	22 100[h]	22 091	$99.6\,^4I_{15/2}+0.39\,^4G_{11/2}+0.05\,^4F_{9/2}$
	451.85	0.31	22 125[h]	22 122	$99.2\,^4I_{15/2}+0.80\,^4G_{11/2}$
	451(b)	0.10	22 166[h]	22 160	$99.8\,^4I_{15/2}+0.20\,^4G_{11/2}$
$^4G_{11/2}$	430.5	0.16	23 224[h]	23 228	$99.7\,^4G_{11/2}+0.27\,^4I_{15/2}+0.05\,^4F_{9/2}$
23 345	428.9	0.25	23 309[h]	23 306	$99.2\,^4G_{11/2}+0.50\,^4I_{15/2}+0.28\,^4F_{9/2}$
	427.8	0.10	23 370[h]	23 369	$98.5\,^4G_{11/2}+1.22\,^4I_{15/2}+0.25\,^4F_{9/2}$
	427.4(sh)	0.05	23 390	23 389	$99.6\,^4G_{11/2}+0.28\,^4I_{15/2}+0.14\,^4F_{9/2}$
	426.9(sh)	0.03	23 420	23 414	$99.6\,^4G_{11/2}+0.36\,^4I_{15/2}+0.15\,^4F_{9/2}$
	426.7(sh)	0.02	23 430	23 427	$99.2\,^4G_{11/2}+0.72\,^4I_{15/2}+0.06\,^4F_{9/2}$

[a]Spectrum obtained at approximately 85 K; the temperature-dependent spectra are not shown.

[b]Multiplet manifold for $Dy^{3+}(4f^9)$; calculated centroid in cm^{-1} is listed below multiplet; transition to $^6F_{1/2}$ too weak to identify without any hot-band data; this multiplet is assumed to be at 13 120 cm^{-1} for purposes of including J-mixing.

[c]Wavelength in nanometers; b denotes broad, sh denotes shoulder.

[d]Intensity in absorbence units.

[e]Experimental energy levels in units of cm^{-1}.

[f]Calculated energy levels in units of cm^{-1} based on B_{nm} parameters: $B_{20}=616$, $B_{40}=-131$, $B_{44}=128$, $B_{60}=46.3$, $B_{64}=641$ (all in cm^{-1}); the DyS polyhedra have D_{2d} symmetry in cubic Th_3P_4.

[g]Based on calculated levels established from B_{nm} parameters listed in footnote f of this table.

[h]Experimental energy levels used in the analysis with the calculated energy levels; 62 experimental to calculated levels yield a final rms deviation of 7 cm^{-1}.

TABLE II. Crystal-field splitting of the ground state, $^6H_{15/2}$.

Level[a]	$E(\mathrm{cm}^{-1})_{\mathrm{abs}}$[b]	$E(\mathrm{cm}^{-1})_{\mathrm{sh}}$[c]	$E(\mathrm{cm}^{-1})_{\mathrm{calc}}$[d]	Percent mixture of states
1	0[e]	0	0.7	$99.9\,^6H_{15/2}+0.04\,^6H_{13/2}+0.03\,^6H_{11/2}$
2	52[e]	65	53	$99.9\,^6H_{15/2}+0.04\,^6H_{13/2}+0.01\,^6F_{7/2}$
3	140[e]	145	124	$99.9\,^6H_{15/2}+0.05\,^6H_{13/2}+0.01\,^6F_{11/2}$
4	190[e]	190	191	$99.9\,^6H_{15/2}+0.06\,^6H_{13/2}+0.02\,^6H_{11/2}$
5	240[e]	240	236	$99.9\,^6H_{15/2}+0.08\,^6H_{13/2}+0.01\,^6F_{11/2}$
6	257[e]	265	246	$99.9\,^6H_{15/2}+0.09\,^6H_{13/2}+0.01\,^6F_{11/2}$
7	310[e]	310	339	$99.9\,^6H_{15/2}+0.06\,^6H_{13/2}+0.04\,^6F_{11/2}$
8	⋯	450	365	$99.9\,^6H_{15/2}+0.04\,^6H_{13/2}+0.04\,^6F_{11/2}$

[a]Each Stark level is twofold degenerate.
[b]Experimental splitting of the ground state based on an analysis of the temperature-dependent spectra observed between 85 K and room temperature.
[c]Schottky levels established from analysis of the heat capacity data obtained from 6 to 350 K. Ref. 19 is the source of data.
[d]Calculated splitting obtained with B_{nm} parameters reported in Table I, footnote f, and experimental levels in Table I (column 4) and Table II (column 2).
[e]Experimental levels used in crystal-field splitting analysis.

The crystal-field Hamiltonian given in Eq. (1) was diagonalized using a truncated basis of states, ^6H_J, ^6F_J, $^4F_{9/2}$, $^4G_{11/2}$, and $^4I_{15/2}$. Within each basis, we calculated the reduced matrix elements in intermediate coupling with the free-ion parameters given by Carnall *et al.*[34] The initial set of B_{nm} parameters was established using the three-parameter theory[35] and lattice-sum monopole components, A_{nm}, assuming that the cation sites filled with Dy^{3+} ions had local polyhedra symmetry of D_{2d}.[30,31]

IV. ANALYSIS OF THE OPTICAL DATA

Tables I and II present the results of a crystal-field splitting analysis of the multiplet manifolds of Dy^{3+} in γ-phase Dy_2S_3. Sixty-two experimental Stark levels were used in the analysis; the rms deviation between the experimental and calculated levels is 7 cm^{-1}. The spectra are generally broader and the individual energy levels are shifted to lower energies than we observe for comparable spectra in fluoride and oxide crystals.[36] This observation known as the ''nephelauxcetic effect'' is associated with an increased covalency in the Dy–S bonds relative to the Dy–F or Dy–O bonds.[37] Further delocalization of the $4f$ orbitals reduces the effective nuclear charge and provides for an overall reduction in the size of the crystal-field splitting.[38]

Table III provides a comparison between the experimental center of gravity (centroid) of the crystal-field split multiplet manifolds of $Dy^{3+}(4f^9)$ in a fluoride host, $Sr_5(PO_4)_3F$,[28] two oxide hosts, Y_2O_3,[29] and $Y_3Sc_2Ga_3O_{12}$ (YSGG),[39] the centroids from Table I, and the centroids from the semiconducting γ-phase Dy_2S_3 crystal reported by Henderson *et al.*[4] The nephelauxcetic shift is pronounced between the first four hosts that are insulators, with the shift toward lower energies from the fluoride, to the oxide, to the sulfide crystal. Furthermore, there is also a reduction in the size of the multiplet manifold splitting. The Dy^{3+} ground-state manifold, $^6H_{15/2}$, has an overall splitting of 1156 cm^{-1} in $Sr_5(PO_4)_3F$, 833 cm^{-1} in Y_2O_3, 614 cm^{-1} in YSGG, and 365 cm^{-1} for Dy_2S_3 predicted in Table II.

Our lattice-sum calculations for Dy^{3+} in the different hosts reported in Table III also provide some interesting in-

TABLE III. Dy^{3+} centroids in insulating and semiconducting crystals.[a]

$^{2S+1}L_J$[b]	$Sr_5(PO_4)_3F$ $E(\mathrm{cm}^{-1})$	Y_2O_3 $E(\mathrm{cm}^{-1})$	YSGG $E(\mathrm{cm}^{-1})$	Dy_2S_3[c] $E(\mathrm{cm}^{-1})$	Dy_2S_3[d] $E(\mathrm{cm}^{-1})$
$^6H_{13/2}$	4394	3900	3717	3668	3413
$^6H_{11/2}$	6763	6205	6030	5918	5842
$^6F_{11/2}$	8524	7984	7840	7604	7625
$^6H_{9/2}$	8676	8075	7900	7988	7836
$^6F_{9/2}$	9764	9318	9188	8918	8900
$^6H_{7/2}$	9999	9449	9269	9388	9178
$^6H_{5/2}$	11 016	10 494	10 357	10 154	10 181
$^6F_{7/2}$	11 776	11 214	11 075	10 945	10 957
$^6F_{5/2}$	13 140	12 597	12 464	12 308	12 315
$^6F_{3/2}$	13 949	12 460	13 266	13 132	13 145
$^4F_{9/2}$	21 829	21 213	21 161	21 101	20 837
$^4I_{15/2}$	22 593	22 203	22 161	22 037	21 926
$^4G_{11/2}$	24 064	23 618	23 431	23 345	Band edge

[a]Established from individual spectra obtained at approximately 85 K.
[b]Multiplet manifold for $Dy^{3+}(4f^9)$.
[c]Centroids reported in Table I from present study.
[d]Centroids reported in Ref. 4 for semiconducting Dy_2S_3.

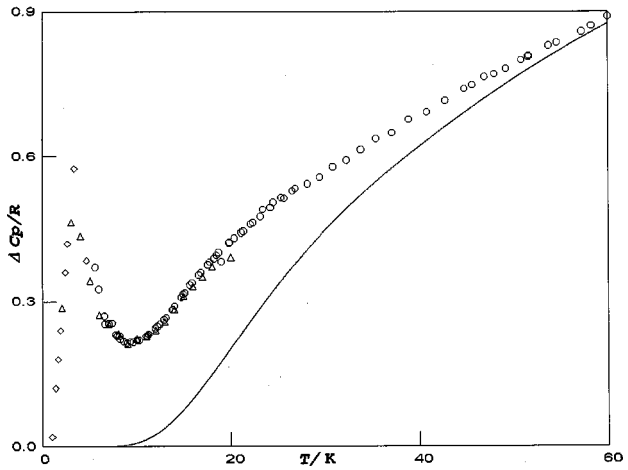

FIG. 1. Plot of $\Delta C_p/R$ against T/K; the data points from Ref. 17 are triangles; data points from Ref. 19 are open circles; reevaluation of data in the present study are open diamonds; magnetic ordering occurs around 3.4 K; remnants of magnetic ordering are identified relative to the solid line (Schottky curve).

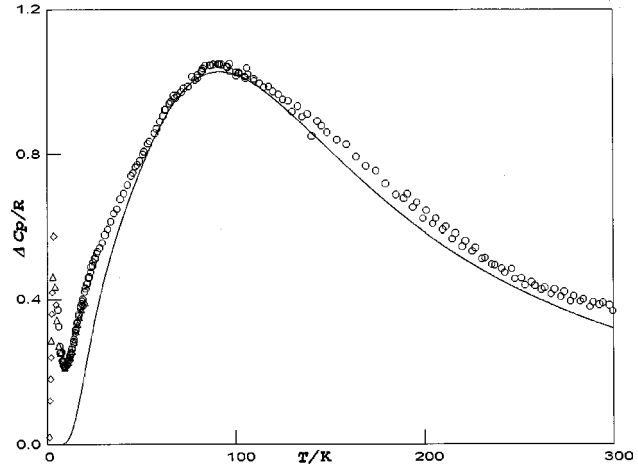

FIG. 2. Plot of $\Delta C_p/R$ against T/K extended to 300 in order to show agreement with the Schottky curve represented as a solid line; data-point symbols are defined in Fig. 1 caption.

sights. The best overall agreement between calculated and observed crystal-field splitting of the $Dy^{3+}(4f^9)$ manifolds in the four different host crystals comes when the formal charge on Dy^{3+} and other ions in the lattice is allowed to vary. In $Sr_5(PO_4)_3F$, best agreement is reached with an effective ionic charge of 3.0 esu on Dy^{3+}. The effective ionic charge decreases to 2.3 esu on Dy^{3+} in the sesquisulfide lattice. This observation is not at odds with the change in bonding character in going from a fluoride to a sulfide host.[37]

Another interesting observation to be made in Table III is that there is not much shift in the centroid energies between the results obtained for Dy^{3+} in the present study and the centroids observed in *n*-type semiconducting γ-phase Dy_2S_3 having a bandgap of 2.94 eV.[4] In the semiconducting crystal, the spectra of the corresponding multiplet manifolds are too broad to carry out a detailed crystal-field splitting analysis. Henderson *et al.*[4] provide an explanation for the observed broadening as due to coulombic scattering of carrier electrons with Dy^{3+} ion sites. Recent temperature-dependent photoconducity measurements using site-selective UV laser excitation into the conduction band edge provide additional experimental support for this mechanism as well.[40,41]

V. ANALYSIS OF THE HEAT CAPACITY DATA

We indicated in the Introduction that one of our objectives was to reconcile the interpretations of the Schottky levels reported by Taher *et al.*[17] and by the Westrum group[19] with the analysis of the crystal-field splitting of the ground state, $^6H_{15/2}$, established from the spectroscopic data reported in the present study. Our source of heat capacity data between 2 and 20 K comes from Taher *et al.*,[17] and between 5 and 350 K the data come from the Westrum group.[19]

To delineate that part of the heat capacity due to the $4f$ electrons, the lattice heat capacity of γ-phase Dy_2S_3 was reevaluated. Using the volumetric approximation, the lattice heat capacity of γ-phase La_2S_3 and Gd_2S_3 were used as the diamagnetic lattice heat capacity anchor points.[18] The molar volumes used were 74.92 (La_2S_3), 66.40 (Gd_2S_3), and 64.58 (Dy_2S_3), in units of cc/mol. The Taher data were evaluated in light of recent data pertaining to the lattice heat capacity of Nd_2O_3 and its relation to similar data for La_2O_3.[42] The lattice heat capacity for Gd_2S_3 was corrected for the splitting of $^8S_{7/2}$ ground state of Gd^{3+} and some remnants of magnetic ordering up to 12 K.

The Schottky and magnetic ordering contributions to the heat capacity are given in Figs. 1 and 2, with Fig. 1 providing greater detail at the lower temperature where magnetic ordering takes place near 3.4 K. The data points of Taher *et al.*[17] are represented as triangles and the data points of the Westrum group are represented as open circles. Reevaluation of both sets of data is reported by symbols appearing as open diamonds in both figures. A smooth function can be established between both sets of data where there is an overlap of temperature. The solid curve represents the Schottky function defined by the eight Kramers doublets of the ground-state manifold, $^6H_{15/2}$ split by the crystal field into Stark levels 0, 65, 145, 190, 240, 265, 310, and 450, all in units of cm^{-1}. The function also includes the assumption that the centroid of the next higher energy-level manifold, $^6H_{13/2}$, which is 14-fold degenerate, is found at 3400 cm^{-1}. The crystal-field splitting of $^6H_{15/2}$ is listed in Table II (column 3).

Table IV reports the integrated reduced entropy (S/R) derived from an analysis of all heat-capacity measurements. This entropy is compared to the entropy derived from the

TABLE IV. Reduced molar entropy of Dy_2S_3.

T/K	S_T^0/R(obs'd)	S_T^0/R(calc'd)
20	1.81	1.56
50	4.41	3.95
100	9.86	9.37
150	14.69	14.19
200	18.61	18.07
300	24.49	23.92

proposed lattice heat capacity and the Stark levels reported in Table II. Implied in this theoretical treatment is the addition of the entropy due to the Kramers degeneracy ($2\ln 2$) of the Stark levels. From a statistical viewpoint this asymptotic value appears at 0 K, but in fact for the lanthanides, it generally comes out in an antiferromagnetic transition not amenable to exact calculation. However, experience has shown that this transition heat is often completed before the Schottky heat capacity maximum. Thus, the observed entropy leads the calculated entropy after 50 K by about 0.5, whereas one would expect these values to coincide here (see Figs. 1 and 2). Our proposed transition curve generates slightly more than the $2\ln 2$ associated with the Kramers degeneracy, but it is still within the experimental error of the measurements involved. This point emphasizes the need for definitive thermal capacity measurements below 15 or 20 K. However, the conclusions drawn from our interpretation of these heat capacities is not on shaky ground. The possibility that twofold degenerate Stark levels are found at 4 and 6 cm^{-1} is not likely. The high temperature Schottky heat capacity would then require all seven doublets of Table II to be sixfold degenerate. This is inconsistent with the $J+1/2$ Stark levels identified from the optical data for the excited $^{2S+1}L_J$ manifolds.

The analysis of the hot-band absorption spectra and the calculated crystal-field splitting given in Table II support the Schottky level assignments of the Westrum group remarkably well for the observed Stark levels of the $^6H_{15/2}$ manifold. The absorption hot bands representing transitions from a Stark level having an energy above 310 cm^{-1} are too weak and broad for analysis.

In conclusion, we find that our interpretation and assignments to the individual Stark levels of the $^6H_{15/2}$ manifold, based on the absorption spectra reported in the present study, are consistent with the Schottky level assignments deduced from analyses of the heat capacity data reported by the Westrum group. Both sets of heat capacity data, however, appear well qualified and consistent; but with the higher temperature heat capacity data and the support from the optical and magnetic studies, it is now possible to interpret the ''bump'' in the heat capacity data at 3.5 K as due to magnetic ordering of a Dy–S polyhedra.

[1] H. J. Goldsmid, in *Applications of Thermoelectricity*, edited by B. L. Worsnop (Mehuen, London, 1960), p. 73.
[2] M. A. Bramson, *Infrared Radiation: A Handbook for Applications* (Plenum, New York, 1971).
[3] A. Yariv and P. Yeh, *Optical Waves in Crystals: Infrared Sensors and Detectors* (Wiley, New York, 1984).
[4] J. R. Henderson, M. Muramato, E. Loh, and J. B. Gruber, J. Chem. Phys. **47**, 3347 (1967).
[5] V. V. Tikhonov and I. A. Smirnov, Fiz. Tverd. Tela (Leningrad) **13**, 2749 (1971) [Sov. Phys. Solid State **13**, 429 (1971)].
[6] V. P. Zhuze, O. A. Golikova, V. M. Sergeeva, and I. M. Rudick, Sov. Phys. Solid State **13**, 669 (1971).
[7] T. Takeda, J. Magn. Magn. Mater. **5**, 315 (1977).
[8] W. A. Zachariasen, Acta Crystallogr. **2**, 57 (1949).
[9] M. Picon, L. Domange, J Flahaut, M. Guittard, and M. Patrie, Bull. Soc. Chim. Fr. **2**, 221 (1960).
[10] M. Atoji, J. Chem. Phys. **54**, 3226 (1971).
[11] R. M. Bozorth, F. Holtzberg, and S. Methfessel, Phys. Rev. Lett. **14**, 952 (1965).
[12] G. Becker, J. Feldhaus, K. Westerholt, and S. Methfessel, J. Magn. Magn. Mater. **6**, 14 (1977).
[13] E. Bucher, K. Andres, F. J. di Salvo, J. P. Malta, A. C. Gossard, A. S. Cooper, and G. W. Hull, Jr., Phys. Rev. B **11**, 500 (1975).
[14] K. A. Gschneidner, Jr., B. J. Beaudry, T. Takeshita, and S. S. Eucher, Phys. Rev. B **24**, 7187 (1981).
[15] I. E. Paukov, V. V. Nogteva, and E. I. Yarembash, Russ. J. Phys. Chem. **43**, 1316 (1969).
[16] E. G. King and W. W. Weller, U.S. Bureau of Mines Bulletin, RI-5485 (1959).
[17] S. M. A. Taher, J. C. Ho, and J. B. Gruber, J. Chem. Phys. **76**, 609 (1982).
[18] E. F. Westrum, Jr., R. Burriel, J. B. Gruber, P. E. Palmer, B. J. Beaudry, and W. A. Plautz, J. Chem. Phys. **91**, 4838 (1989).
[19] J. B. Gruber, R. Burriel, E. F. Westrum, Jr., W. Plautz, G. Metz, X-X. Ma, B. J. Beaudry, and P. E. Palmer, J. Chem. Phys. **95**, 1964 (1991).
[20] R. Shaviv, E. F. Westrum, Jr., J. B. Gruber, B. J. Beaudry, and P. E. Palmer, J. Chem. Phys. **96**, 6149 (1992).
[21] J. R. Henderson, M. Muramato, J. B. Gruber, and R. Menzel, J. Chem. Phys. **52**, 2311 (1970).
[22] J. B. Gruber, R. P. Leavitt, and C. A. Morrison, J. Chem. Phys. **79**, 1664 (1983).
[23] V. P. Zhuze, A. A. Kamarzin, M. G. Karin, K. K. Sidorin, and A. I. Shelykh, Sov. Phys. Solid State **21**, 1968 (1979).
[24] R. Burriel, Instituto de Ciencia de Materiales de Aragón, Universidad de Zaragoza-CSIC, 5009 Zaragoza, Spain, 1989 (unpublished).
[25] J. R. Henderson, M. Muramato, E. Loh, D. M. Johnson, and J. B. Gruber, ''Purification and Growth of Rare-Earth Compound Semiconductors,'' DAC-59368P (McDonnell-Douglas Astronautics, Santa Monica, CA), 1969.
[26] J. B. Gruber, Portland State University, Portland, OR, 1984 (unpublished).
[27] C. A. Morrison, *Angular Momentum Theory Applied to Interactions in Solids, Lecture Notes in Chemistry* (Springer, New York, 1988).
[28] J. B. Gruber, B. Zandi, and L. Merkle, J. Appl. Phys. **83**, 1009 (1998).
[29] N. C. Chang, J. B. Gruber, R. P. Leavitt, and C. A. Morrison, J. Chem. Phys. **76**, 3877 (1982).
[30] A. A. Kaminskii, Phys. Status Solidi A **102**, 389 (1987).
[31] B. J. Beaudry and P. E. Palmer, Ames Laboratory, Iowa State University, Ames, IA, 1980 (unpublished).
[32] C. A. Morrison, R. P. Leavitt, and D. E. Wortman, J. Chem. Phys. **73**, 2580 (1980).
[33] C. A. Morrison and R. P. Leavitt, J. Chem. Phys. **71**, 2366 (1979).
[34] W. T. Carnall, P. R. Fields, and K. Rajnak, J. Chem. Phys. **49**, 4412 (1968).
[35] R. P. Leavitt, C. A. Morrison, and D. E. Wortman, ''Three-Parameter Theory of Crystal Fields,'' Harry Diamond Laboratories Technical Report, HDL-TR-1673, No. 3, June, 1975, Adelphi, MD.
[36] C. A. Morrison and R. P. Leavitt, in *Handbook on the Physics and Chemistry of Rare Earths*, edited by K. A. Gschneidner, Jr. and L. Eyring (North-Holland, New York, 1982), Vol. 5, p. 461.
[37] C. K. Jørgensen, *Orbitals in Atoms and Molecules* (Academic, New York, 1962).
[38] B. G. Wybourne, *Spectroscopic Properties of Rare Earths* (Wiley Interscience, New York, 1965).
[39] M. D. Seltzer, A. O. Wright, C. A. Morrison, D. E. Wortman, E. D. Filer, and J. B. Gruber, J. Phys. Chem. Solids **57**, 1175 (1996).
[40] L. C. Olsen, S. M. A. Taher, and J. B. Gruber, J. Chem. Phys. **60**, 2050 (1974).
[41] J. B. Gruber, San Jose State University, San Jose, CA, 1997 (unpublished).
[42] J. B. Gruber, B. Zandi, B. H. Justice, and E. F. Westrum, Jr., manuscript in preparation, 1999.